JACS
JOURNAL OF THE AMERICAN CHEMICAL SOCIETY
Article
pubs.acs.org/JACS

Multiferroic Materials Based on Organic Transition-Metal Molecular Nanowires

Menghao Wu,*[,†,‡,§] J. D. Burton,[§] Evgeny Y. Tsymbal,[§] Xiao Cheng Zeng,[‡] and Puru Jena[†]

[†]Department of Physics, Virginia Commonwealth University, Richmond, Virginia 23284, United States
[‡]Department of Chemistry and [§]Department of Physics and Astronomy, University of Nebraska, Lincoln, Nebraska 68588, United States

Supporting Information

ABSTRACT: We report on the density functional theory aided design of a variety of organic ferroelectric and multiferroic materials by functionalizing crystallized transition-metal molecular sandwich nanowires with chemical groups such as −F, −Cl, −CN, $-NO_2$, =O, and −OH. Such functionalized polar wires exhibit molecular reorientation in response to an electric field. Ferroelectric polarizations as large as 23.0 $\mu C/cm^2$ are predicted in crystals based on fully hydroxylized sandwich nanowires. Furthermore, we find that organic nanowires formed by sandwiching transition-metal atoms in croconic and rhodizonic acids, dihydroxybenzoquinone, dichloro-dihydroxy-*p*-benzoquinone, or benzene decorated by −COOH groups exhibit ordered magnetic moments, leading to a multiferroic organometallic crystal. When crystallized through hydrogen bonds, the microscopic molecular reorientation translates into a switchable polarization through proton transfer. A giant interface magnetoelectric response that is orders of magnitude greater than previously reported for conventional oxide heterostructure interfaces is predicted.

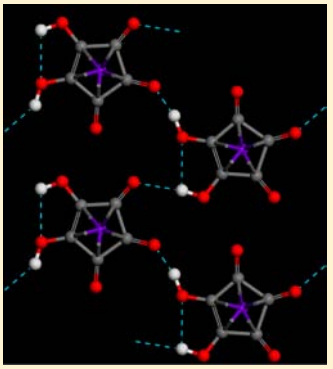

INTRODUCTION

Ferroelectric materials, whose spontaneous electric polarizations can be switched under an external electric field, have a wide range of applications.[1] The first ferroelectric crystal, Rochelle salt, which contains organic tartrate ion, was discovered in 1920.[2] Recent discoveries of ferroelectricity in organic solids have been limited to some well-known polymer ferroelectrics,[3] such as polyvinylidene difluoride (PVDF),[4−11] and a few low molecular mass compounds, such as thiourea,[12] tetrathiafulvalene (TTF) complexes with *p*-bromanil (tetrabromo-*p*-benzoquinone)[13] and *p*-chloranil (tetrachloro-*p*-benzoquinone),[14] croconic acid (CA)[15] and so on. Synthesis of new organic ferroelectric materials that are light, flexible, and nontoxic will have important applications in the field of organic electronics. Multiferroics where magnetism and ferroelectricity coexist are even more desirable for constructing multifunctional devices[16−22] since charges can be controlled by applied magnetic fields and spins by applied voltages. Single-phase multiferroic materials, however, are rare as magnetic and electrical ordering arise from competing interactions that are difficult to incorporate in the same compound, let alone in organic multiferroic materials.[23−25]

Ferrocene, $Fe(C_5H_5)_2$, is a molecule composed of an Fe atom sandwiched between two parallel cyclopentadienyl (Cp) rings. Since its discovery in 1950,[26] ferrocene-like molecular complexes,[27−30] where the central Fe atom is replaced by other metal atoms and one-dimensional (1D) transition-metal molecular sandwich nanowires (SNWs), have attracted considerable attention because of their intriguing magnetic properties and potential applications in electron transport and spin filtering.[31−42] Various ferrocene-like dicyclopentadienyl complexes, such as VCp_2, $CrCp_2$, $MnCp_2$, $CoCp_2$, $NiCp_2$, and $ZnCp_2$ as well as larger transition-metal molecular complexes, e.g., seven-decker $V_7(Bz)_8$ sandwich clusters and eighteen-decker $Eu_{18}(C_8H_8)_{19}$ nanorods, have been successfully synthesized in the laboratory.[27−29] Similarly, multidecker transition-metal benzene (Bz) sandwich complexes, $[M_n(Bz)_m$ (M = Sc−Ni)] have also been reported.[28,29] First-principles calculations have predicted that some of these transition-metal benzene (MBz) or transition-metal cyclopentadienyl (MCp) SNWs, such as $[Fe(Cp)]_\infty$, $[Mn(Bz)]_\infty$, or $[V(Bz)]_\infty$, are ferromagnetic and may exhibit half metallicity, i.e., conducting in one spin channel while insulating in the other spin channel. These have promising applications as nanoscale spin filters with high transmission spin polarization. Some SNWs, such as $[Cr(Bz)]_\infty$ and $[Mn(Cp)]_\infty$, which are nonmagnetic, may even become magnetic or half-metallic upon charge injection.[39]

We report here on several SNWs which are modified by various chemical functional groups such that they may possess electric dipole moments and therefore may serve as ferroelectric materials. Because some of these complexes are predicted to be ferromagnetic, coexistence of magnetism and ferroelectricity is expected, thus leading to the synthesis of organic multiferroics. We also discuss two different mechanisms, namely, molecular reorientation and proton transfer that give rise to ferroelectricity.

Received: May 1, 2012
Published: August 10, 2012

dx.doi.org/10.1021/ja304199x | J. Am. Chem. Soc. 2012, 134, 14423−14429

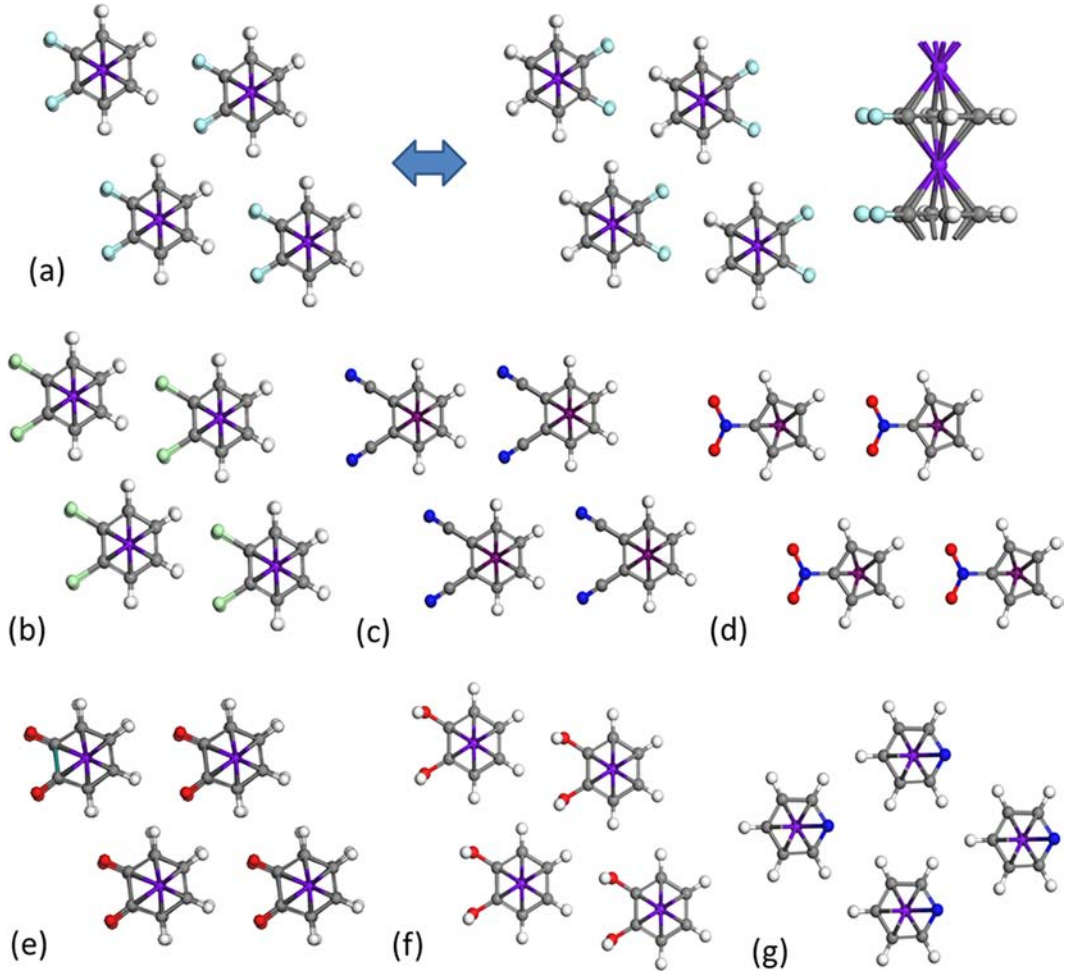

Figure 1. Crystal structures of VBz or VCp SNWs decorated by (a) −F; (b) −Cl; (c) −CN; (d) $-NO_2$; (e) =O; (f) −OH; and (g) V atoms sandwiched between pyridines. Gray, white, purple, dark-blue, red, bright-blue, and green spheres denote C, H, V, N, O, F, and Cl atoms, respectively.

COMPUTATIONAL DETAILS

First-principles calculations based on the density functional theory (DFT) are carried out using the Vienna ab Initio Simulation Package (VASP5.2).[43−45] Projector augmented wave (PAW) potentials for the core and Perdew−Burke−Ernzerhof (PBE) form[46] of the generalized gradient approximation (GGA) to the exchange−correlation functional are used. Each supercell contains two formula units: two organic molecules and two transition-metal atoms. The size of supercell as well as atomic positions are optimized until the forces are below 0.01 eV/Å. The kinetic energy cutoff is set to be 500 eV, and the Brillouin zone is sampled by using 3 × 3 × 10 k points in the Monkhorst−Pack scheme.[47] The Berry phase method was employed to evaluate the crystalline polarization.[48,49] Some of the calculations of charge analysis, dipole moments of molecules, and vibration frequency are performed by using Dmol^3 4.4 package.[50,51]

RESULTS AND DISCUSSIONS

Our first design of an organic ferroelectric involved the functionalization of MBz SNWs by substituting two adjacent hydrogen atoms in every Bz molecule by two fluorine atoms. The resulting 1,2-difluorobenzene (DFBz) has an in-plane net dipole moment of 3.0 D (1 D = 3.336×10^{-30} C·m) oriented perpendicular to the F side of the DFBz. Using vanadium (V) and the β-phase of the PVDF[12] crystal as a prototype structure, we constructed a V intercalated difluorobenzene (VDFBz) SNW polymer crystal. The optimized structure is shown in Figure 1a. The nearest H−F distance between adjacent parallel SNWs is 2.55 Å. The cohesive energy of −0.29 eV per supercell (−0.145 eV per formula unit) is comparable to that of the β-phase of PVDF (−0.24 eV).[12]

Realizing that in weakly bonded systems standard DFT/GGA calculations do not provide accurate energies due to lack of treatment of dispersive forces, we have carried out additional calculations of the cohesive energy (E_{coh} = E (crystal) − E (SNW), where E(crystal) is the total energy of the SNW crystal per supercell, and E(SNW) is the total energy of a single nanowire per supercell) using the PBE-D2 functional of Grimme[52] that takes into account dispersive forces. Our computed cohesive energy per formula unit using this method is −0.72 eV, which is substantially larger than that obtained using the PBE functional. We have also repeated this calculation using local density approximation which is known to overbind and often compensates for the lack of dispersive forces. This yields a cohesive energy of −0.46 eV. This provides us with more confidence that the organic multiferroic material we have designed is indeed stable and can be potentially synthesized.

We have also studied some other possible crystal structures by changing the directions of the dipole moments between two nearest DFBzs along the chains in increments of 60° (see Figure S1a−c, Supporting Information). The extreme case of

dx.doi.org/10.1021/ja304199x | J. Am. Chem. Soc. 2012, 134, 14423−14429

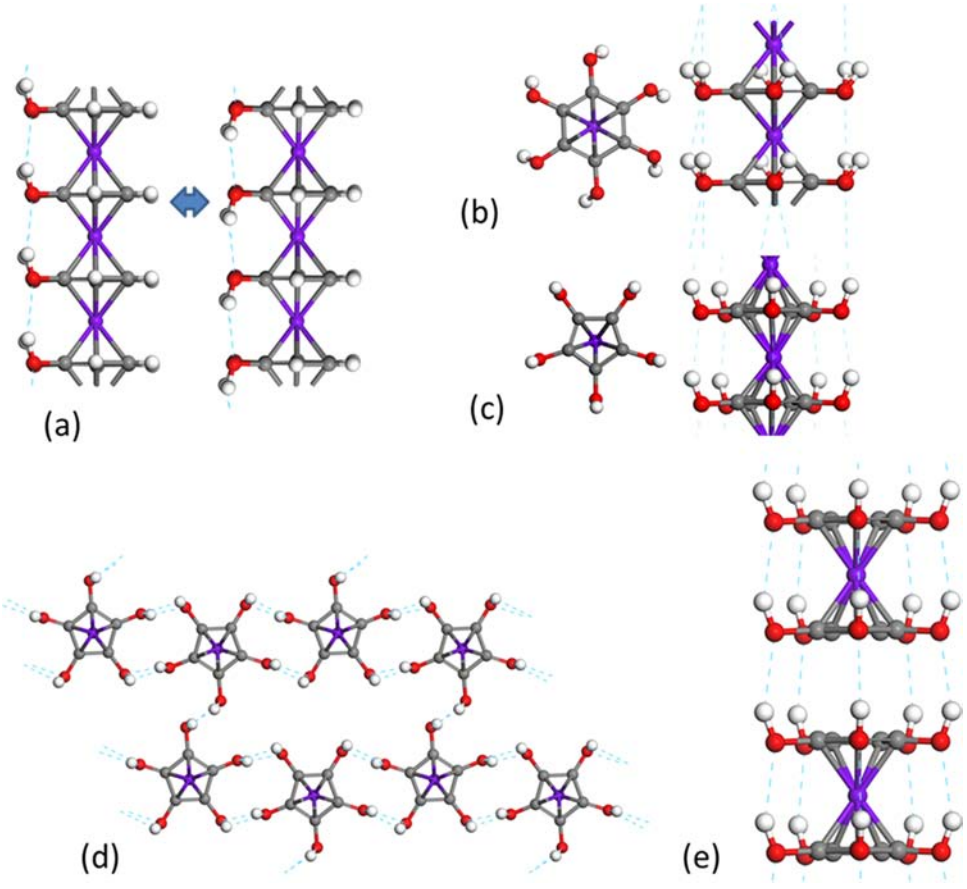

Figure 2. (a) Partially and fully hydroxylized and (b) MBz and (c) MCp SNWs. (d) A fully hydroxylized MnCp SNW crystal structure and (e) a SNW composed of hydrogen-bonded ferrocene-like dicyclopentadienyl complex. Blue dashed lines denote hydrogen bonds.

neighboring moments rotated by 180° (Figure S1c) corresponds to antiferroelectric ordering, whereas the structure in Figure S1a corresponds to ferroelectric ordering. Figure S1d corresponds to another configuration of antiferroelectric ordering which is centrosymmetric. Each of these structures is higher in energy than the ferroelectric state by 0.37, 0.41, 0.05, and 0.84 eV per supercell, respectively. Vibration frequency calculations were also performed, and no imaginary frequencies were found, confirming that the ferroelectric structure in Figure 1a is stable. In addition to the rhombohedral supercells shown in Figure 1, we also examined a tetragonal structure (Figure S1e) which was found to be higher in energy by 0.41 eV per supercell, indicating that the lower symmetry rhombohedral supercell is preferred. The optimized structure of crystallized VDFBz of finite length along SNW direction (see Figure S1f) is also stable without imaginary frequency. Further, we performed quantum molecular dynamics simulation and found the system to be stable at 300 K. The details of these results are given in Figure S1g.

The transition-metal 3d orbitals are split under the D_{6h} crystal field symmetry into a d_{z^2} (a_1) band and two sets of doubly degenerate d_{xy}, $d_{x^2-y^2}$ (e_2) and d_{xz}, d_{yz} (e_1) bands as indicated in the band structure plot in Figure S2a. In crystallized VDFBz SNWs D_{6h} symmetry is broken by the introduction of −F and therefore lifts the degeneracy of the e_2 and e_1 orbital manifolds, as shown in Figure S2b. Since neighboring parallel SNWs are well-separated, the band structure near the Fermi level is quite flat for directions perpendicular to the SNW axis. Hence the crystal is essentially insulating along the polarization direction, opening the possibility that an electric field can reverse the direction of dipole moment through reorientation of the DFBzs, similar to the case of PVDF.[5−12] The dipole moment of the VDFBz SNW crystal, according to our Berry phase calculations, is 11.0 μC/cm^2 which is comparable to that of PVDF, namely, 15 μC/cm^2. The magnetic moment on each V is 0.5 μ_B, and the ground state is ferromagnetic, indicating multiferroic behavior of our VDFBz SNW structures.

This approach to exploring organometallic SNWs is not limited to the structures described above, and indeed a wealth of similar compounds can be imagined. For example, to see if larger dipole moments are possible, we have decorated the Bz molecules by replacing H with larger halogen atoms, such as −Cl (Figure 1b), or other chemical functional groups like −CN, −NO_2, =O, −OH (Figure 1c−f). Similarly, one can also replace V by other transition-metal elements, such as Sc, Ti, Cr, and Mn, or one can replace the Bz ring with Cp or pyridine rings (Figure 1d,g). The sandwiched molecules in Figure 1a−c,e,f are, respectively, difluorobenzene, dichlorobenzene, dicyanobenzene, benzoquinone, and catechol, which are well-known in organic chemistry. According to our calculations, the dipole moments of the decorated molecules sandwiched between metal atoms in Figure 1b−g on the horizontal plane are 2.3, 7.2, 5.5, 6.5, 0.8, and 2.3 D, respectively. Thus, much larger dipole moments can be achieved by replacing F with −CN, −NO_2, and =O ligands in Figure 1c−e. The polarizations corresponding to molecular crystals are 13.7, 18.5, and 22.1 μC/cm^2, respectively. Note that in Figure 1f each

dx.doi.org/10.1021/ja304199x | J. Am. Chem. Soc. 2012, 134, 14423−14429

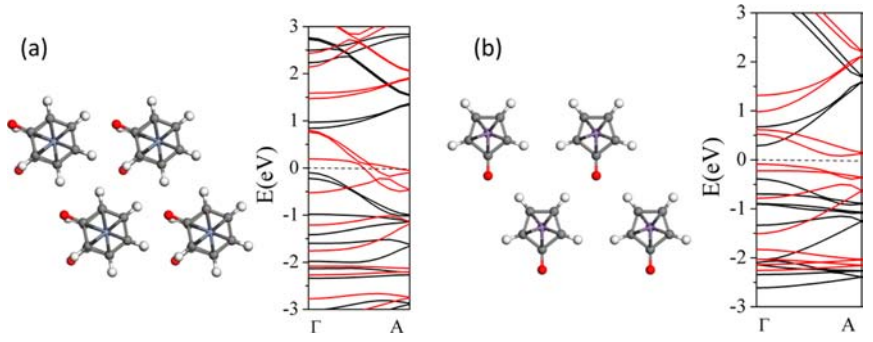

Figure 3. Geometrical and band structures of crystallized (a) CrBz-1O and (b) MtCp-1O SNWs. Black and red curves correspond to majority and minority spins.

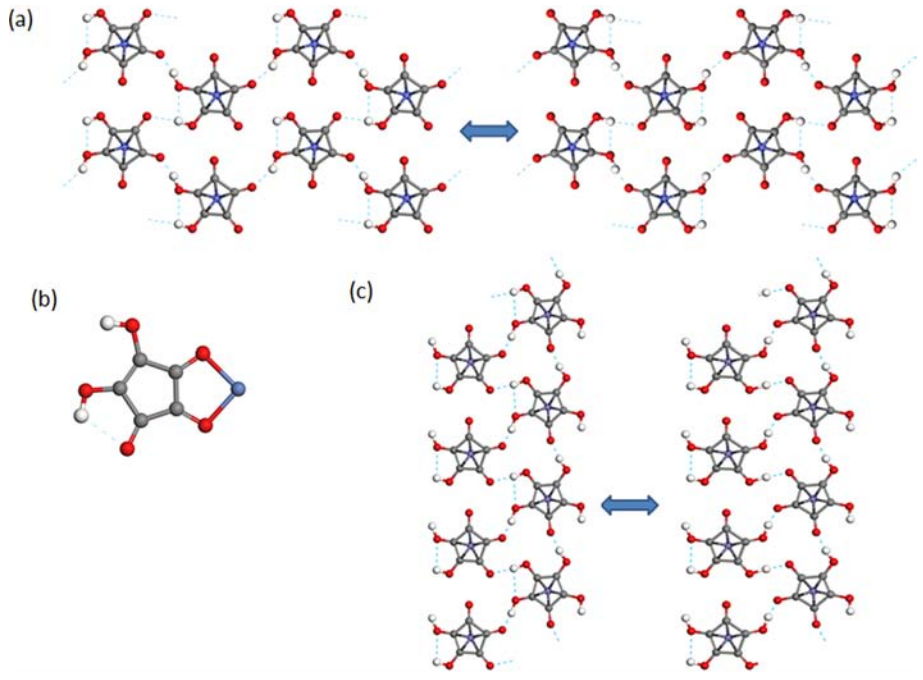

Figure 4. Structures of (a) crystallized MCA SNWs; (b) M attached to CA molecule; metal atom (M) is in blue; and (c) two hydrogen-bonded arrays of MCA SNWs with protons between them.

hydroxyl group can form hydrogen bonds with another hydroxyl group on the adjacent catechol. As a result, the hydrogen atom in each hydroxyl group will not stay in the catechol plane. Consequently, every catechol has a dipole moment of 2.9 D perpendicular to the catechol plane and hence can be switched under an applied electric field (see Figure 2a). If every Bz or Cp in a SNW is fully decorated by hydroxyl groups, as shown in Figure 2b,c, each of them would have a dipole moment of 7.3 D. These are, however, only ferroelectric when the SNWs are insulating along the SNW axis. We studied various SNWs and found only CrBz, MnCp, and TiBz SNWs to be truly insulating. In fully hydroxylized MnCp crystals, where SNWs are connected by hydrogen bonds, as shown in Figure 2d, we find a polarization of 23.0 μC/cm^2. This is even larger than the 21 μC/cm^2 polarization found in CA.[15] CrBz and MnCp SNWs are nonmagnetic, while TiBz SNWs are antiferromagnetic. Another option is to hydroxylize stable ferrocene-like dicyclopentadienyl complexes, such as VCp_2, $CrCp_2$, and $MnCp_2$, so that they can form insulating SNWs through self-assembly by forming hydrogen bonds. This is shown in Figure 2e and possesses both magnetism and ferroelectricity.

We investigated the compositional dependence of magnetism in SNWs by decorating the Bz and Cp rings with different ligands. For pristine VBz SNWs the magnetic moment on each V atom is 0.95 μ_B. According to Hirshfeld charge analysis, every V atom carries a positive charge of 0.12 e. For the systems in Figure 1a,c,e,f where SNWs are decorated with −F, −CN, =O, and −OH, the magnetic moments of every V atom are 0.5, 1.0, 1.9, and 0.85 μ_B, respectively. The respective charges on V atoms are 0.08, 0.15, 0.24, and 0.09 e. According to previous work,[33] magnetism of the intercalated metal atom can be tuned by charge injection. Groups, such as −F and −OH, that reduce charge on the V atom lead to a lower magnetic moment, while groups, such as −CN and =O, that enhance the positive charge on V also enhance its magnetic moment, in agreement with ref 33. Thus, one can tune the magnetic moment on the metal atom by changing its charge through ligand decoration. Note that the change in the magnetic moment is the largest when Bz is decorated with an =O ligand. We denote it as Bz-1O since one π-electron is removed from six available π-

dx.doi.org/10.1021/ja304199x | J. Am. Chem. Soc. 2012, 134, 14423−14429

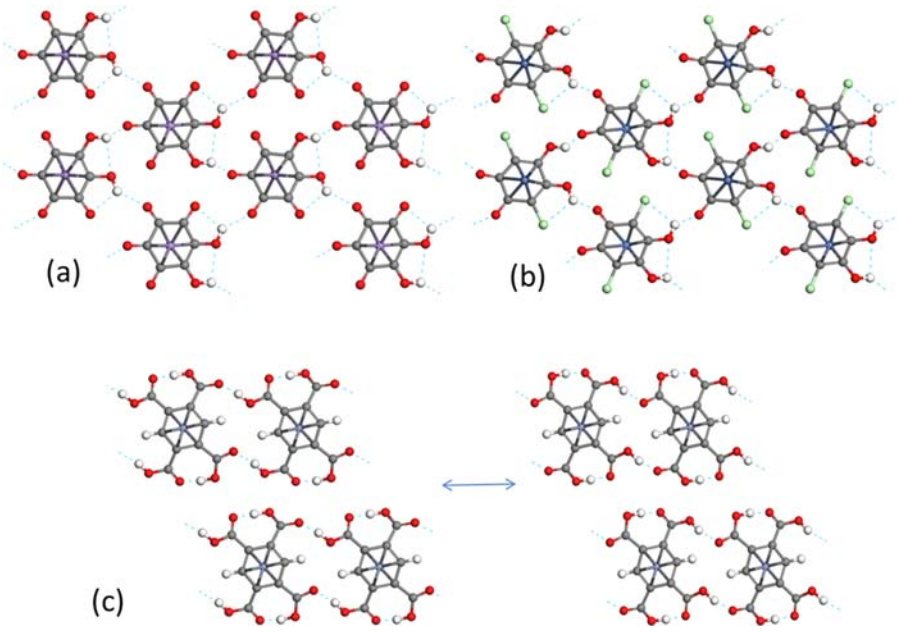

Figure 5. Crystal structures of (a) MRA, (b) M-dichloro-dihydroxy-*p*-benzoquinone SNWs, and (c)VBz SNWs decorated by hydrogen-bonded −COOH groups.

electrons of Bz because of the double bond. According to the Huckel rule, the Bz-1O tends to capture an extra electron to form a stable aromatic configuration having $4m + 2$ electrons. So adding an ═O is similar to replacing Bz by Cp or removing an electron from each cell. To verify this, we consider[33] the nonmagnetic SNWs CrBz and MnCp, both with e_2 and a_1 orbitals completely occupied and e_1 unoccupied in both spin channels. In the case of CrBz with a charge injection of 1e per Cr atom, i.e., CrCp or CrBz-1O, the magnetic moment on every Cr atom is about 1.0 μ_B. Similarly, MnCp, MnBz-1O, or MnBz SNWs with charge injection of 1 e per Mn atom is nonmagnetic, while MnCp-1O or MnCp SNWs with charge injection of 1 e per Mn atom is ferromagnetic. The magnetic moment on every Mn atom is around 1.0 μ_B in both the systems.

The geometries and band structures of crystallized CrBz-1O and MnCp-1O SNWs, which are transformed from completely nonmagnetic to magnetic configurations by functional decoration, are displayed in Figure 3. CrBz-1O becomes a half metal, while MnCp-1O is a magnetic semiconductor with a band gap of 0.17 eV. When protons are attached to ═O groups of CrBz-1O and MnCp-1O SNWs they become hydroxyl groups. The corresponding SNWs both become nonmagnetic, as expected from the change in charge state.

In a recent article room temperature ferroelectricity was reported in crystalline CA,[15] with a large spontaneous polarization of 21 $\mu C/cm^2$. The application of an external electric field to this lattice of hydrogen-bonded molecules leads protons associated with one molecule to shift to a hydrogen-bonded neighbor and, therefore, causes the molecular dipoles to switch. Hence, a large switchable polarization was realized in an organic crystal without any molecular reorientation. Subsequently some other hydrogen-bonded organic ferroelectrics with smaller polarizations have also been fabricated and studied theoretically,[53,54] suggesting that hydrogen-bonded ferroelectrics have many merits and that the design principle can be much more simple compared to conventional organic ferroelectrics.[55]

Motivated by this discovery, we replaced the Bz or Cp in crystalline MBz/MCp SNWs by CA molecules to study the possible coexistence of magnetism and ferroelectricity. We denote such a metal-CA system as MCA. As shown in Figure 4a, we studied M = Sc−Ni but found only systems with M = Fe, Co, and Ni to be stable without any imaginary frequencies. The cohesive energies of MCA SNWs (E_{coh} = E(SNW) − E(M) − E(CA), where E(M) and E(CA) are the total energy of a single metal atom and CA molecule, respectively) are −2.3, −2.4, and −2.6 eV for M = Fe, Co, and Ni, respectively. These are more stable than those of metal atoms that directly bind with two ═O groups on every CA, as shown in Figure 4b, where the corresponding binding energies of the metal atom are −1.7, −1.8, and −2.1 eV, respectively. The cohesive energy due to hydrogen bonds among SNWs is all around −1.08 eV per supercell (−0.54 eV per formula unit) which is much higher than that of the β-phase of PVDF (−0.24 eV). The calculated polarizations for M = Fe, Co, and Ni are, respectively, 20.5, 23.7, and 20.5 $\mu C/cm^2$. These are approximately the same as that of the CA crystal, namely, 21.0 $\mu C/cm^2$ (ref 15). The magnetic moments on Fe, Co, and Ni are, respectively, 1.3, 0.3, and 0.0 μ_B. Here FeCA and CoCA crystals are ferromagnetic and, thus, multiferroic.

As mentioned above, when a proton is attached to ═O forming MBz-1O or MCp-1O, the magnetic moment on M will change significantly. Here, proton transfer not only can switch polarization but also can tune the magnetic properties of MCA SNWs. In Figure 4c we consider a bilayer sheet consisting of two layers of MCA SNWs where two protons per unit cell are placed between two chains of MCA SNWs. The magnetic moments of an MCA SNW (M = Fe, Co, and Ni) with two protons attached to each CA are, respectively, 0.6, 0.4, and 0.0 μ_B. We note that while for Co and Ni there is almost no change in the magnetic moment, the moment at Fe is reduced by almost half. Thus, in FeCA SNW proton transfer not only causes the polarization to switch from left to right but also causes a "transfer" of magnetic moment of 0.7 μ_B on each Fe atom. If the right chain has M = Co or Ni and the left chain has

dx.doi.org/10.1021/ja304199x | J. Am. Chem. Soc. 2012, 134, 14423−14429

Fe, an external applied electric field will move the protons from the left to the right chain, thus enhancing the total magnetic moment of the system, respectively, by 0.8 and 0.7 μ_B per unit cell. The surface magnetoelectric coefficient, α_s, is defined in terms of the change in the surface (interface) magnetization ΔM in response to electric field E, as $\mu_0 \Delta M = \alpha_s E$.[56] For the Fe(001) film surface,[56] α_s was found to be 2.4×10^{-14} Gcm^2/V. It is enhanced significantly in the presence of a dielectric with a high dielectric constant, and for the $SrTiO_3/SrRuO_3$ interface, α_s is predicted to become 2.0×10^{-12} Gcm^2/V.[57] If a ferroelectric material is used as one of the constituents of the heterostructure, the response becomes nonlinear, but as a figure of merit the magnetoelectric response can be estimated as the ratio of ΔM to the coercive field of ferroelectric. For $BaTiO_3$/Fe,[58,59] $BaTiO_3/Co_2MnSi$,[60] $BaTiO_3/Fe_3O_4$,[61] and $BaTiO_3/SrRuO_3$,[62] values of α_s of the order of 10^{-10} Gcm^2/V have been predicted. Assuming the required electric field for proton transfer in MCA to be same as that in pure CA, namely, 37 kV/cm as in ref 15, we find $\alpha_s \approx 1.0 \times 10^{-9}$ Gcm^2/V. This is nearly 40 000, 500, and 10 times larger than the magnitude of α_s for the Fe(001) film surface,[56] $SrTiO_3/SrRuO_3$ interface,[57] and $BaTiO_3$/ferromagnetic metal interfaces,[58−62] respectively.

In addition to CA, another good candidate material may be synthesized by substituting the Bzs or Cps in crystalline MBz/MCp SNWs by rhodizonic acid (RA). We denote this structure as MRA, as shown in Figure 5a. The dipole moment of MRA may also be reversed through intermolecular proton transfer. From the frequency analysis, however, we find that only systems with M = Co or Ni are stable. The magnetic moments on Co and Ni are, respectively, 0.5 and 0.0 μ_B, and the ground state is ferromagnetic when M = Co. Thus, CoRA is the only multiferroic material. The MRA systems with M = V, Cr, Mn, Fe, Co, and Ni can be stabilized by replacing two =O groups on every RA with −H or −Cl. The resulting dihydroxybenzoquinone and dichloro-dihydroxy-*p*-benzoquinone structures are displayed in Figure 5b. The magnetic moments on V, Cr, Mn, Fe, Co, and Ni are, respectively, 1.9, 2.0, 1.0, 0.0, 1.0, and 0.0 μ_B, in which those with nonzero net magnetic moments are all ferromagnetic, making all systems but Fe and Ni multiferroic.

We have also examined whether −COOH ligands can lead to ferroelectricity by intermolecular proton transfer. As shown in Figure 5c, when every Bz in a VBz SNWs crystal is decorated by four −COOH groups, they form hydrogen-bonded arrays. Here, the proton can transfer from one −COOH to the adjacent −COOH allowing the dipole moment to switch under an external electric field. Such proton transfer in hydrogen-bonded −COOH chains can find its prototype in the CBDC studied in ref 53. With a calculated polarization of 10.9 μC/cm^2 and a magnetic moment of 1.0 μ_B on every V atom in ferromagnetic ground state, the system is multiferroic. In Figure S3 we studied two hydrogen-bonded finite clusters taken from −COOH decorated VBz SNWs. This system has a large dipole moment of 35 D.

CONCLUSIONS

In summary, using first-principle calculations we predict that crystallized MBz and MCp SNWs may become ferroelectric or even multiferroic as the organic molecules are decorated with −F, -Cl, −CN, $-NO_2$, =O, or −OH. A polarization as high as 23.0 μC/cm^2 is achieved in fully hydroxylized MnCp SNWs. We also show that the magnetic moment of transition-metal atoms can be changed by appropriate choice of ligands. Multiferroelectricity may be achieved when the benzene molecules are replaced by CA, RA, dihydroxybenzoquinone, or dichloro-dihydroxy-*p*-benzoquinone. Similar results can also be obtained when Bz is decorated by −COOH groups, as this allows the polarization to switch by proton transfer between hydrogen-bonded neighbors. A high surface magnetoelectric coefficient that is several orders of magnitude larger than previously reported is predicted. This study provides new pathways to the synthesis of organic ferroelectric and multiferroic materials with potential applications, including many hydrogen-bonded systems that are likely to be fabricated through self-assembly.

ASSOCIATED CONTENT

Supporting Information

Different structures of DFBzs and bandstructures are collected. This material is available free of charge via the Internet at http://pubs.acs.org.

AUTHOR INFORMATION

Corresponding Author

mwu2@vcu.edu

Notes

The authors declare no competing financial interest.

ACKNOWLEDGMENTS

The work is supported by the National Science Foundation through the Nebraska EPSCoR (NSF grant no. EPS-1010674) and the Nebraska MRSEC (NSF grant no. DMR-0820521). P.J. acknowledges partial support by the Department of Energy. Computations are performed at the University of Nebraska Holland Computing Center.

REFERENCES

(1) Scott, J. F. *Ferroelectric Memories*: Springer-Verlag: Berlin, Heidelberg, Germany, 2000.
(2) Valasek, J. *Phys. Rev.* **1920**, *15*, 537.
(3) Sachio, H.; Yoshinori, T. *Nat. Mater.* **2008**, *7*, 357.
(4) Fukada, E. *IEEE Trans.* **2000**, *47*, 1277.
(5) Yasuhiro, Y.; Tadokoro, H. *Macromolecules* **1980**, *13*, 1318.
(6) Poly(Vinylidene Fluoride) (PVDF) and its Copolymers. In *Encyclopedia of Smart Materials*; Zhang, Q. M., Bharti, V., Kavarnos, G., Schwartz, M., Eds.; Wiley: New York, 2002; Vols. *1* and *2*, pp 807−825.
(7) Bune, A. V.; Fridkin, V. M.; Ducharme, S.; Blinov, L. M.; Palto, S. P.; Sorokin, A. V.; Yudin, S. G.; Zlatkin, A. *Nature* **1998**, *391*, 874.
(8) Tasaka, S.; Miyata, S. *Ferroelectrics* **1981**, *32*, 17.
(9) Nix, E. L.; Ward, I. M. *Ferroelectrics* **1986**, *67*, 137.
(10) Tashiro, K.; Kobayashi, M.; Tadokoro, H.; Fukada, E. *Macromolecules* **1980**, *13*, 691.
(11) Pei, Y.; Zeng, X. C. *J. Appl. Phys.* **2011**, *109*, 093514.
(12) Goldsmith, G. J.; White, J. G. *J. Chem. Phys.* **1959**, *31*, 1175−1187.
(13) Tokura, Y.; Koshihara, S.; Iwasa, Y.; Okamoto, H.; Komatsu, T.; Koda, T.; Iwasawa, N.; Saito, G. *Phys. Rev. Lett.* **1989**, *63*, 2405.
(14) Okamoto, H.; Mitani, T.; Tokura, Y.; Koshihara, S.; Komatsu, T.; Iwasa, Y.; Koda, T.; Saito, G. *Phys. Rev. B* **1991**, *43*, 8224.
(15) Horiuchi, S.; Tokunaga, Y.; Giovannetti, G.; Picozzi, S.; Itoh, H.; Shimano, R.; Kumai, R.; Tokura, Y. *Nature* **2010**, *463*, 789.
(16) Cheong, S.; Mostovoy, M. *Nat. Mater.* **2007**, *6*, 13.
(17) Ramesh, R.; Spaldin, N. A. *Nat. Mater.* **2007**, *6*, 21.
(18) Eerenstein, W.; Mathur, N. D.; Scott, J. F. *Nature* **2006**, *442*, 759−765.
(19) Wang, K. F.; Liu, J. M.; Ren, Z. F. *Adv. Phys.* **2009**, *58*, 321.
(20) Vaz, C. A. F.; Hoffman, J.; Ahn, C. H; Ramesh, R. *Adv. Mater.* **2010**, *22*, 2900.

(21) Ma, J.; Hu, J.; Li, Z.; Nan, C.-W. *Adv. Mater.* **2011**, *23*, 1062.
(22) Velev, J. P.; Jaswal, S. S.; Tsymbal, E. Y. *Philos. Trans. R. Soc.* **2011**, *369*, 3069.
(23) Giovannetti, G.; Kumar, S.; Stroppa, A.; Brink, J.; Picozzi, S. *Phys. Rev. Lett.* **2009**, *103*, 266401.
(24) Jain, P.; Ramachandran, V.; Clark, R. J.; Zhou, H. D.; Toby, B. H.; Dalal, N. S.; Kroto, H. W.; Cheetham, A. K. *J. Am. Chem. Soc.* **2009**, *131*, 13625−13627.
(25) Kagawa, F.; Horiuchi, S.; Tokunaga, M.; Fujioka, J.; Tokura, Y. *Nat. Phys.* **2010**, *6*, 169.
(26) Kealy, T. J .; Pauson, P. L. *Nature* **1951**, *168*, 1039.
(27) Hedberg, L.; Hedberg, K. *J. Chem. Phys.* **1970**, *53*, 1228.
(28) Gard, E.; Haaland, A.; Novak, D.P .; Seip, R. *J. Organomet. Chem.* **1975**, *88*, 181.
(29) Almenningen, A.; Gard, E.; Haaland, A. *J. Organomet. Chem.* **1976**, *107*, 273.
(30) Kandalam, A. K.; Rao, B. K.; Jena, P.; Pandey, R. *J. Chem. Phys.* **2004**, *120*, 10414.
(31) Kurikawa, T.; Takeda, H.; Hirano, V; Judai, K.; Arita, T.; Nagao, S.; Nakajima, A.; Kaya, K. *Organometallics* **1999**, *18*, 1430.
(32) Hosoya, N.; Takegami, R.; Suzumura, J.; Yada, K.; Koyasu, K.; Miyajima, K.; Mitsul, M.; Knickelbein, M. B.; Yabushita, S.; Nakajima, A. *J. Phys. Chem. A* **2005**, *9*, 109.
(33) Xiang, H. J.; Yang, J. L.; Hou, J. G.; Zhu, Q. S. *J. Am. Chem. Soc.* **2006**, *128*, 2310.
(34) Maslyuk, V.. V.; Bagrets, A.; Meded, V.; Arnold, A.; Evers, F.; Brandbyge, M.; Bredow, T.; Mertig, I. *Phys. Rev. Lett.* **2006**, *97*, 09720.
(35) Koleini, M.; Paulsson, M.; Brandbyge, M. *Phys. Rev. Lett.* **2007**, *98*, 197202.
(36) Atodiresei, N.; Dederichs, P. H.; Mokrousov, Y.; Bergqvist, L.; Bihlmayer, G.; Blugel, S. *Phys. Rev. Lett.* **2008**, *100*, 117207.
(37) Zhou, L.; Yang, S. W.; Ng, M.; Sullivan, M. B.; Tan, V. B. C.; Shen, L. *J. Am. Chem. Soc.* **2008**, *130*, 4023.
(38) Shen, L.; Yang, S. W.; Ng, M.-F.; Ligatchev, V.; Zhou, L.; Feng, Y. J. *J. Am. Chem. Soc.* **2008**, *130*, 13956.
(39) Wu, M.; Zeng, X. C. *Appl. Phys. Lett.* **2011**, *99*, 053121.
(40) Zhang, X.; Wang, J. L.; Gao, Y.; Zeng, X. C. *ACS Nano* **2009**, *3*, 537.
(41) Zhang, Z.; Wu, X.; Guo, W.; Zeng, X. C. *J. Am. Chem. Soc.* **2010**, *132*, 10215.
(42) Wu, X.; Zeng, X. C. *J. Am. Chem. Soc.* **2009**, *131*, 14246.
(43) Kresse, G.; Hafner, J. *Phys. Rev. B* **1993**, *47*, 558.
(44) Kresse, G.; Furthmuller, J. *Phys. Rev. B* **1996**, *54*, 11169.
(45) Kresse, G.; Joubert, D. *Phys. Rev. B* **1999**, *59*, 1758.
(46) Perdew, J. P.; Burke, K.; Ernzerhof, M. *Phys. Rev. Lett.* **1996**, *77*, 3865.
(47) Monkhorst, H. J.; Pack, J. D. *Phys. Rev. B* **1976**, *13*, 5188.
(48) King-Smith, R. D.; Vanderbilt, D. *Phys. Rev. B* **1993**, *47*, 1651.
(49) Resta, R.; Posternak, M.; Baldereschi, A. *Phys. Rev. Lett.* **1993**, *70*, 1010.
(50) Delley, B. *J. Chem. Phys.* **1990**, *92*, 508−517.
(51) Delley, B. *J. Chem. Phys.* **2000**, *113*, 7756−7764.
(52) Grimme, S. *J. Comp. Chem. Soc.* **2006**, *27*, 1787−1799.
(53) Horiuchi, S.; Kumai, R.; Tokura, Y. *Adv. Mater.* **2011**, *23*, 2098.
(54) Stroppa, A.; Sante, D.; Horiuchi, S.; Tokura, Y.; Vanderbilt, D.; Picozzi, S. *Phys. Rev. B* **2011**, *84*, 014101.
(55) Poulsen, M.; Ducharme, S. *IEEE Trans. Dielectr. Electr. Insul.* **2010**, *17* (4), 1028.
(56) Duan, C. G.; Velev, J. P.; Sabririanov, R. F.; Zhu, Z.; Chu, J.; Jaswal, S. S.; Tsymbal, E. Y. *Phys. Rev. Lett.* **2008**, *102*, 137201.
(57) Roondinelli, J. M.; Stengel, M.; Spaldin, N. A. *Nat. Nanotechnol.* **2008**, *3*, 46.
(58) Duan, C. G.; Jaswal, S. S.; Tsymbal, E. Y. *Phys. Rev. Lett.* **2006**, *97*, 047201.
(59) Fechner, M.; Maznichenko, I. V.; Ostanin, S.; Ernst, A.; Henk, J.; Bruno, P.; Mertig, I. *Phys. Rev. B* **2008**, *78*, 212406.
(60) Yamauchi, K.; Sanyal, b.; Picozzi, S. *Appl. Phys. Lett.* **2007**, *91*, 062506.
(61) Niranjan, M. K.; Velev, J. P.; Duan, C. G.; Jaswal, S. S.; Tsymbal, E. Y. *Phys. Rev. B.* **2008**, *78*, 104405.
(62) Niranjan, M. K.; Burton, J. D.; Velev, J. P.; Jaswal, S. S; Tsymbal, E. Y. *Appl. Phys. Lett.* **2009**, *95*, 052501.